Synergistic effects of *Ret* coding and enhancer loss-of-function alleles cause progressive loss of inhibitory motor neurons in the enteric nervous system

Lauren E Fries,[1] Gabriel Grullon,[1] Hanna E Berk-Rauch,[1] Aravinda Chakravarti,[1,2,#] and Sumantra Chatterjee[1,2,#]

[1] Center for Human Genetics & Genomics, [2] Department of Neuroscience and Physiology, New York University Grossman School of Medicine, New York, NY 10016

 # Send all correspondence to:

Sumantra Chatterjee, Ph.D.
Center for Human Genetics & Genomics
New York University Grossman School of Medicine
435 East 30th Street, Room 1012
New York, NY 10016
(212) 263-8029
sumantra.chatterjee@nyulangone.org

Aravinda Chakravarti, Ph.D.
Center for Human Genetics & Genomics
New York University Grossman School of Medicine
435 East 30th Street, Room 802/3
New York, NY 10016
(212) 263-8023
aravinda.chakravarti@nyulangone.org

ORCID IDs:
LEF: 0000-0003-3148-440X
GG: 0009-0002-4842-5238
HBR: 0000-0002-1238-1248
AC: 0000-0002-4264-2285
SC: 0000-0002-5076-1698

Abstract

Coding and enhancer variants of the *RET* receptor tyrosine kinase gene contribute to ~50% of Hirschsprung disease (HSCR) risk, a congenital disorder of disrupted enteric nervous system (ENS) development. The greatest contribution of this risk is from a common variant (rs2435357) in an ENS-active, SOX10-bound *RET* enhancer (MCS+9.7) that reduces *RET* gene expression *in vivo* and triggers expression changes in other ENS genes in the human fetal gut. To uncover the cellular basis of *RET*-mediated aganglionosis, we used CRISPR/Cas9 to delete (Δ) the homologous mouse enhancer (mcs+9.7). We used single cell RNA sequencing and high-resolution immunofluorescence to demonstrate four significant features of the developing E14.5 gut of Δmcs+9.7/Δmcs+9.7 embryos: (1) a small (5%) yet significant reduction in *Ret* gene expression in only two major cell types – early differentiating neurons and fate-restricted inhibitory motor neurons; (2) no significant cellular loss in the ENS; and, (3) loss of expression of 19 cell cycle regulator genes suggesting a proliferative defect. To identify the *Ret* functional threshold for normal ENS development, we also generated, in combination with the *Ret* CFP null allele, (4) Δmcs+9.7/CFP double heterozygote mice which reduced *Ret* gene expression in the ENS to 42% with severe loss of inhibitory motor neurons, an effect restricted to the hindgut and driven by proliferative loss. Thus, *Ret* gene expression drives proliferation of ENS progenitor cells and hindgut-specific inhibitory motor neuron development, and that HSCR aganglionosis arises from a cascade of cellular defects triggered by >50% loss of *Ret* function.

Introduction

The enteric nervous system (ENS), the largest component of the peripheral nervous system, is composed of a ganglionic network of over 600 million neurons innervating the entire gastrointestinal (GI) tract (Furness, 2012). This network is formed by the cranio-caudal proliferation, differentiation and migration of Enteric Neural Crest-derived Cells (ENCDCs) in the developing gut across weeks 4 to 8 in the human and embryonic day (E) 10.5 to E14.5 in the mouse embryo (Furness, 2012). One of the key genes involved in this developmental process is the receptor tyrosine kinase RET (Natarajan et al., 2002; Uesaka et al., 2008), whose expression in ENCDCs promotes proliferation and cell survival, although the gene is more broadly expressed in other tissues (e.g., kidney, brain, dorsal root ganglia). Significantly, coding and non-coding *RET* deficiency mutations lead to isolated Hirschsprung disease (HSCR) in ~50% of cases, a rare (~1/5,000 live births) developmental disorder of the ENS characterized by the absence of enteric ganglia along variable lengths of the distal bowel (Alves et al., 2013; Tilghman et al., 2019). In the developing mouse gut, *Ret* deficiency leads to significant transcriptional changes affecting numerous transcription factors (TFs), signaling molecules, and specific transport and biosynthesis genes, leading to aganglionosis (Chatterjee et al., 2019; Heanue and Pachnis, 2006). Analogous genetic changes are observed in the *RET* deficient human fetal gut carrying HSCR-associated susceptibility alleles in multiple *RET* enhancers (Chatterjee et al., 2023).

The cell type-specific phenotype of *Ret* loss-of-function (LoF) has primarily been studied in *Ret* null homozygote mouse models (Lasrado et al., 2017; Vincent et al., 2023), which demonstrate that complete *Ret* deficiency leads to precocious differentiation and reduction in the number of proliferating ENCDCs leading to these cells' inability to access the inhibitory motor neuron program (Vincent et al., 2023). *Ret* heterozygous mice do not exhibit aganglionosis in the developing gut or have any other phenotypes associated with *Ret* LoF (Kapoor et al., 2017; Vincent et al., 2023), although *Ret* heterozygotes in combination with hypomorphic homozygote mutations in the epistatic endothelin type B receptor gene (*EDNRB*) causes variable aganglionosis (Carrasquillo et al., 2002; McCallion et al., 2003).

In the human, most HSCR patients have heterozygous *RET* variants, some of which are complete LoF but most are hypomorphic; additionally, most patients harbor both *RET* coding and enhancer variants while yet other carry rare and common variants in other ENS and gut mesenchymal genes that are members of a large *RET-EDNRB* gene regulatory network (GRN) (Tilghman et al., 2019). Thus, we hypothesize that the totality of cis and trans sequence variants in an individual that reduce *RET* gene expression to less than 50% of wildtype levels lead to functional *RET* haploinsufficiency and aganglionosis.

To address this hypothesis, we focus here on mouse models of HSCR with both coding and regulatory *RET* variants. Specifically, we first generated a mouse model by targeting an intronic enhancer of *Ret* (mcs+9.7) whose human homolog is the SOX10-bound *RET* enhancer (MCS+9.7) that harbors a common (24% - 45%) allele that individually increases HSCR risk 4-fold (Emison et al., 2010; Emison et al., 2005). Other *RET* enhancers also harbor polymorphic HSCR-associated variants which can cumulatively increase risk by 10-fold or greater (Chatterjee et al., 2021). Functionally, the common risk allele at MCS+9.7 disrupts SOX10 binding and leads to loss of *RET* function both in neural crest derived neuroblastoma cell lines (Chatterjee et al., 2021) as well as in the human fetal gut (Chatterjee et al., 2023). In addition, we also generated Δmcs+9.7/+; CFP/+ compound heterozygote mice by crossing the enhancer disrupted mice with a well characterized *Ret* null heterozygote mouse (*Ret*$^{+/CFP}$) (Uesaka et al., 2008; Vincent et al., 2023), to study the progressive cellular defects arising from the coding and non-coding *Ret* variants.

To characterize these mice with decreasing levels of *Ret* gene expression we used single cell (sc) RNA-seq coupled with spatial transcriptomics and immunofluorescence of the E14.5 mouse gut. Enhancer deletion homozygotes showed 5% reduction in *Ret* gene expression as well as in other cell type-specific transcriptional changes in the ENS but with no reduction in cell numbers or cell types. However, double heterozygote mice demonstrated significant reduction (to 42%) in *Ret* gene expression but only in inhibitory motor neurons (iMNs) and a glial cell population expressing progenitor markers. This was accompanied by loss in cell numbers only in the iMNS in the distal hindgut but spared the

glial population. This cell loss is mediated by the reduced proliferative capacity of these cells, providing a mechanistic basic for aganglionosis.

Our studies highlight that the HSCR phenotype results from precise thresholding of *Ret* gene expression in specific cell types in specific regions of the developing gut, requiring at least 50% gene expression for normal gut development. These results provide a basis for understanding the genotype-phenotype correlation and HSCR penetrance for different *RET* and other gene mutations in HSCR.

Results

Deletion of a HSCR-associated Ret enhancer in mice leads to loss of Ret expression in vivo

The MCS+9.7 *RET* enhancer, harboring the HSCR-associated common variant rs2435357, is sequence conserved in mice and other vertebrates including the zebrafish (Emison et al., 2005; Grice et al., 2005), and functions as a *RET* enhancer in mouse and zebrafish transgenic assays (Chatterjee et al., 2016; Grice et al., 2005). MCS+9.7 binds SOX10 and regulates the expression of *RET* in human cell lines and the human fetal GI tract (Chatterjee et al., 2023; Chatterjee et al., 2021). First, we assessed the ability of this enhancer to regulate cell-type specific *Ret* expression in the developing mouse gut by deleting a 183 bp segment of the conserved region (Chr6:118,164,102-118,163,917; mm10) centered on the Sox10 binding site within the first intron of *Ret* (**Figure 1A**). We measured gene expression of *Ret* in the developing mouse gut (foregut, caecum, and hind gut) at E12.5 and E14.5, the migratory and proliferative stages of ENS development, using quantitative real time PCR (qRT-PCR). There were no measurable changes in *Ret* expression in heterozygote deleted mice (Δmcs+9.7/+) at either developmental stage, but a small (5%) yet significant (p<0.01) reduction in Δmcs+9.7/Δmcs+9.7 homozygotes (**Figure 1B**). To determine if the enhancer regulated *Ret* at birth, we measured *Ret* expression at postnatal time 0 (P0) in the small intestine and colon, the tissues derived from the foregut and hind gut. We detected a similar 5% (p<0.01) decrease in *Ret* expression in homozygotes as in development (**Figure 1B**). Thus, the 183bp DNA element is sufficient to act as an *in vivo* developmental enhancer of *Ret* in the gut.

We also generated double heterozygote mice carrying both the Δmcs+9.7 and a *Ret* coding deletion allele by breeding with the *Ret* CFP null mutation (**Methods** (Vincent et al., 2023)), i.e., +/Δmcs+9.7; +/CFP. These latter mice retained, on average, 42% (p<0.01) of *Ret* gene expression in the developing gut as compared to the wildtype at both developmental stages and at birth (**Figure 1C**). In previous studies, we demonstrated that reduction of *Ret* gene expression to 50% does not lead to any major transcriptional or cellular changes in the developing GI tract as compared to wildtype embryos (Kapoor et al., 2017; Vincent et al., 2023) but complete *Ret* LoF leads to severe cellular defects and prenatal lethality (Uesaka et al., 2008), limiting the utility of the LoF mouse model alone to dissect *Ret* function and HSCR pathophysiology. Hence, the double heterozygote *Ret* genotype is a useful strain to ask whether 42%, as opposed to 50%, of *Ret* gene expression alters gut cell composition in any meaningful way. We also ascertained the tissue specificity of this enhancer by measuring gene expression of *Ret* in the developing kidney, an organ whose development is dependent on the correct spatio-temporal expression of *Ret* (Schuchardt et al., 1994). There are no detectable changes in *Ret* expression in Δmcs+9.7/Δmcs+9.7 embryonic kidneys at either E12.5 or E14.5 but a 50% reduction in +/Δmcs+9.7;+/CFP mice, reflecting the loss of *Ret* gene expression from the heterozygous *Ret* knockout alone with no detectable additional contribution from the deleted enhancer (**Supplementary Figure 1**) . Thus mcs+9.7 primarily controls *Ret* expression in the ENCDCs of the developing gut and fate committed ENS at birth.

To validate if the observed transcriptional changes in the wildtype, Δmcs+9.7/Δmcs+9.7, and +/Δmcs+9.7; +/CFP are reflected in the corresponding protein levels *in situ*, we performed immunofluorescence on the whole gut tube for all three genotypes at E14.5. *Ret* gene expression in the migrating ENCDCs was significantly reduced only in +/Δmcs+9.7; +/CFP embryos (p < 0.01) as compared to wildtype embryos, leading to loss of migrating ENCDCs in the terminal end of the hindgut near the anal pore (**Figure 1D**). There are no measurable cellular changes in Δmcs+9.7/Δmcs+9.7 mice while *Ret* null (CFP/CFP) mice demonstrated a near complete lack of ENCDCs as previously reported (Vincent et al., 2023). To determine if this cellular effect due to reducing *Ret* expression is maintained at birth, we stained the descending colon, the derivate of the hind gut, with Acetylcholinesterase (AChE), the primary cholinergic enzyme found at postsynaptic

neuromuscular junctions, and routinely used as a diagnostic marker for aganglionosis in humans (Yoshimaru et al., 2021) and the mouse (Kapoor et al., 2017; McCallion et al., 2003). We observed significantly reduced cholinergic neuron fibers in the distal colon of +/Δmcs+9.7; +/CFP P0 mice reminiscent of short segment HSCR, with normal innervation observed only in wildtype and Δmcs+9.7/Δmcs+9.7 P0 colons (**Supplementary Figure 2**).

Specific ENS transcriptional and cellular changes from functional loss of a Ret enhancer

We next explored which gut-specific cell type the enhancer was active in. To do so, we performed single cell RNA-seq on dissected foregut and hindgut (below the stomach to the anal pore) at E14.5, the developmental stage when ENS migration through the gut is complete and ENS cells have started differentiating into neuronal and glial subclasses. We studied tissues from each of two wildtype and two Δmcs+9.7/Δmcs+9.7 homozygote embryos to collect 25,028 wildtype and 35,505 Δmcs+9.7/Δmcs+9.7 homozygote single cells (**Methods**). From these data we identified 3,415 high-variability genes and 20 principal components (PCs) to cluster cells based on their differential gene expression (FDR<0.05) across clusters, relative to the mean expression in other clusters. We used marker genes to specify the identity of each cluster as follows: Smooth muscle (*Acta2, Actg2, Myh11*; 32 % of cells), Epithelial (*Epcam, Cldn7, Lgals4*; 11%), Extra cellular matrix/Fibroblast (*Adamec1, Col6a4, Col3a1*; 30%), Endothelial (*Lars2, Tagln2*; 2%), Immune (*C1qa, C1qb, Cd52*; 2%), ENS (*Ret, Ednrb, Ngfr, Tubb3*; 11%) and a class of undifferentiated but transcriptionally active cells which have yet to acquire any major recognizable cell fate (*H9, Hmga2,Hoxa9*; 11%) (**Figure 2A**).

Overall, there is no significant deviation in cell type composition between the wildtype and the Δmcs+9.7/Δmcs+9.7 GI tract (p=0.18; hypergeometric test) (**Figure 2B**). This is not surprising given that only 5% of *Ret* expression is lost in this genotype and that our prior studies with heterozygous *Ret* LoF mice (CFP/+) with 50% loss of *Ret* expression are overall phenotypically normal (Vincent et al., 2023). Thus, we asked whether any changes were evident in specific cell types, particularly across *Ret* expressing cells. Differential gene expression analysis across genotypes and clusters identified 97 genes that were significantly

affected by homozygous enhancer loss (FDR<0.1) of which 74 (60 downregulated and 14 upregulated, or 76%) were altered in the ENS cluster only; the remaining 23 (20 downregulated and 3 upregulated) genes were differentially expressed in the epithelial cluster, the only other non-ENS cell type where *Ret* is detectably expressed. Within the ENS cluster, *Ret* demonstrates 8% reduced expression (p<0.001) highlighting the specificity of the mcs+9.7 *Ret* enhancer (**Figure 2C**). Among the 74 ENS genes affected, 51 were specific neuronal markers, including the glutaminergic neuronal gene *Grin2b* (1.67-fold lower in the enhancer null, FDR<0.01), the interneuron markers *Scrt1* and *Nxph4* (1.28- and 1.37-fold reduced in the enhancer null, respectively) and the inhibitory motor neuron markers *Vip* and *Nos1* (0.6- and 0.8-fold lower in the enhancer null, respectively) (FDR<0.01 for all results). In previous transcriptional studies of complete *Ret* null mice guts, we had discovered 520 genes that were significantly (FDR<0.01) affected in *Ret* expressing cells of the ENS (Vincent et al., 2023); of these, 48 genes are in common with the 74 affected in the Δmcs+9.7/Δmcs+9.7 ENS, albeit to a much smaller extent as expected (**Supplementary Figure 3**), although not affecting cell composition. In other words, even a 5% decrease in *Ret* gene expression affects the *same network of genes* that are affected in a *Ret* LoF homozygotes but with an attenuated response.

Since the ENS is the primary site of action for the *Ret* mcs+9.7 enhancer, we analyzed these cells in greater detail. The ENS cells we captured in our single cell experiments comprise 6 major cell types: (1) ENS progenitors with significantly higher expression (>2-fold; FDR<0.05) of neural crest (NC) markers (e.g., *Sox10, Ednrb, Zeb2*) as well as glial markers (e.g., *Plp1*); (2) differentiating neurons and glia expressing pan neuronal and pan glial markers, such as, *Snap25, Plp1, Mpz,* along with dorsal Hox transcription factors like *Hoxd5 and Hoxd6*; (3) inhibitory motor neurons expressing *Nos1* and *Vip*; (4) excitatory motor neurons expressing *Calb2* and *Chat*; (5) interneurons expressing *Scrt1, Nxph4* and *Dlx5;* and, (6) cholinergic neurons expressing *Chat* and *Slc18a3* (**Figure 2D**). These genes mark a developmental trajectory starting with progenitor cells that lead to more mature neuronal subtypes at the tip of the manifold with an intermediate state of actively dividing and differentiating neurons (**Figure 2D**). To ascertain if the identified subclusters truly represent a developmental trajectory, we used their gene expression patterns to perform a

formal trajectory analysis using *Monocle 3* (Trapnell et al., 2014) which tests whether gene expression is associated with pseudo-time by fitting additive models of gene expression as a function of pseudo-time. This unsupervised reconstruction analysis does indicate that ENS cells follow the expected developmental path along the manifold from undifferentiated (placed at time 0) to more mature neuronal cells (**Figure 2E**).

Given *Ret*'s role in initiating differentiation of ENCDCs to a more mature neuronal fate (Natarajan et al., 2002), our results demonstrate that its expression is absent from the progenitor cells at E14.5, with robust expression detected in all other sub clusters (**Figure 2F**). Despite its broad expression pattern in the developing ENS, in Δmcs+9.7/Δmcs+9.7 homozygotes, loss of expression is limited to a 4-fold (p<0.05) downregulation in differentiating neurons and glia and a 2.3-fold (p<0.05) downregulation in inhibitory motor neuron cells, as compared to wildtype cells (**Figure 2F**). These results demonstrate a biphasic cell type-specific control of *Ret* by the mcs+9.7 enhancer restricted to early differentiating cells and to a very specific class of neurons. Subsequently, although we can observe an effect on the overall transcriptional program in these cells from loss of enhancer activity, there is no detectable *cellular phenotype*, with identical proportions of cells detected in all clusters in both variant genotypes (**Figure 2G**).

Coding and non-coding Ret variants lead to specific cellular defects in the ENS

A key question in HSCR is how lowering *Ret* gene expression levels below a threshold in the ENS lead to disease penetrance. It is clear that HSCR-associated variants within *RET* enhancers, and other enhancers at *NRG1* and *SEMA3* (Jiang et al., 2015), have lower penetrance than pathogenic *RET* coding variants, with the highest penetrance induced by *RET* null mutations (Tilghman et al., 2019). Indeed, disease segregation (penetrance) in some multiplex HSCR families can be better explained from the combined effects of coding and non-coding mutations at *RET* (Emison et al., 2010), reducing gene expression below a threshold. Therefore, we ascertained the effect of such double heterozygote mutations (Δmcs+9.7, +/+, CFP) on the transcription and cellular architecture of the developing mouse gut. We dissociated cells from the hindguts and foreguts of two such embryos for a total of 31,244 cells. After stringent quality control (**Methods**), we used 28,181 cells for

two-dimensional embedding (UMAP) using 2,000 high-variance genes incorporating 20 PCs. These cells were classified into the same 7 cell types as previously annotated (**Figure 2A**) and did not show any deviation from expected numbers of cells per cluster when compared to either wildtype or the Δmcs+9.7/Δmcs+9.7 homozygote (FDR= 0.19; hypergeometric test).

Given that *Ret*'s role during GI development is primarily restricted to the ENS, we therefore assessed 9,760 ENS cells in greater detail from all three genotypes, namely, wildtype (n = 3,752 cells), Δmcs+9.7/Δmcs+9.7 (n = 3,183 cells), and +/Δmcs+9.7; +/CFP (n = 2,825 cells). These cells were re-clustered using 1,654 high variance genes and 20 PCs: we obtained eight clusters corresponding to the six major ENS cell types we detected previously (**Figure 3A**). Combining cells from all 3 genotypes afforded us greater resolution to identify ENS cell subtypes since we could impute missing gene expression from the larger numbers of cells per cluster. The six clusters were annotated based on marker gene expression as Progenitor/Glia: (cluster 0: *Plp1, Mpz,* cluster 1: *Foxd3, Fabp7,* cluster 4: *Mest, S100b),* differentiating neuron and glia (cluster 2: *Cxcl12, Nkain4, Ednrb, Sox10,*), inhibitory motor neurons (cluster 3: *Nos1, Vip*), cholinergic neurons (cluster 5: *Slc10a4, Chrnb2*), interneurons (Cluster 6: Scrt1, Dlx5, Nxph4) and excitatory motor neurons (Cluster 7: *Calb2, Chat*). We then asked if decreased *Ret* expression below 50% had any effect on any ENS cell type. Using a chi-squared test for equality of cell proportions, we observed significant depletion of inhibitory motor neurons (39% lower: FDR = $3x10^{-8}$) and differentiating neurons and glia (34% lower: FDR = $2.2x10^{-4}$) in +/Δmcs+9.7; +/CFP embryos as compared to the wildtype; all other clusters has expected numbers of cells (progenitor cells: p = 0.4, excitatory neurons: p = 0.18, cholinergic neurons: p = 0.3, and interneurons: p = 0.3) (**Figure 3B, C**). This cell depletion is observed in both embryos (replicates) increasing our confidence that this is not an artifact of cell sampling.

Given the increasing evidence pointing to the critical role of iMNs in ENS development (Morarach et al., 2021), and its specific loss attributed to aganglionosis in multiple animal models, including models of *Ret* deficiency (Kuil et al., 2023; Spencer et al., 2021; Vincent

et al., 2023), we investigated if cellular loss of this cell type is a direct consequence of loss of *Ret* expression from its lowered enhancer activity. We calculated the proportions of cells which co-expressed both *Ret* and *Sox10*, the transcription factor bound to the mcs+9.7 enhancer, given Sox10's role in regulating genes involved in maintaining progenitor/glial identity (Bondurand and Sham, 2013; Paratore et al., 2002). Note that 88% of Sox10-expressing cells are in the progenitor or differentiating neurons and glia cluster (**Figure 3D**); conversely, 74% of *Ret*-expressing cells are specific lineage-committed neuronal cells of inhibitory (41%), excitatory (16%), cholinergic (12%) and interneurons (5%) (**Figure 3D**), highlighting *Ret*'s role in maintaining overall neuronal identity in the ENS (Natarajan et al., 2002). This analysis revealed that in inhibitory motor neurons 83% of all cells co-express both genes, but only 18%, 2%, 0.4 % and 0.2% of differentiating neurons and glia, interneurons, excitatory motor neurons and cholinergic neurons, respectively, co-express *Ret* and *Sox10* (**Figure 3D**). We detected no cells co-expressing these genes in progenitor cells (**Figure 3D**). Since reduced expression of *Ret* dysregulates feedback to *Sox10*, and both are critical drivers of aganglionosis in HSCR (Chatterjee et al., 2016; Chatterjee et al., 2021; Chatterjee et al., 2019), this suggest that iMNs and differentiating neurons and glia, which express both *Ret* and *Sox10*, are the primary cell types affected in HSCR.

Ret deficiency induces specific transcriptional changes in inhibitory motor neurons

Given the significant cellular loss observed in iMNs in +/Δmcs+9.7; +/CFP embryos, we investigated the transcriptional profile of these neurons in greater detail by assessing them separately from the rest of the ENS cells (**Figure 4A**). These cells express the classical iMN markers *Nos1, Vip, Gal* and *Ntng1*, which have been previously shown to establish the developmental trajectory towards the iMN fate in the ENS by us and others (Morarach et al., 2021; Vincent et al., 2023) (**Figure 4B**). Given the observed cellular loss, we thus measured their gene expression changes and showed that *Nos1, Vip* and *Gal* were reduced by 2.8-fold, 1.6-fold and 1.3-fold (FDR<0.01 for all tests) in +/Δmcs+9.7; +/CFP embryos while *Ntng1* was unaffected (**Figure 4C**). In Δmcs+9.7/Δmcs+9.7 embryos only *Vip* and *Nos1* were reduced by 0.6 and 0.8-fold (FDR<0.01 for both) but we detected no significant change in expression of either *Gal* or *Ntng1* (**Figure 4C**). We next assessed if this gene expression and cellular loss, observed in our single cell sequencing data, is recapitulated *in*

vivo. Thus, we performed immunofluorescence staining for nNOS and Vip in wildtype and +/Δmcs+9.7; +/CFP embryonic guts at E14.5. While wildtype embryos demonstrated uninterrupted neuronal connections along the entire length of the gut, both *Nos1* and *Vip* positive neurons were significantly reduced but only at the distal end of the hindgut near the future anal pore (**Figure 4D**). Additionally, while *Nos1* positive neurons, though reduced in numbers, presented with normal morphology, *Vip* positive neurons were clumped together in the distal hindgut (**Figure 4D**), a hallmark of loss of proliferative and migratory capacity which has been previously observed in surviving ENCDCs of *Ret* null embryos (Hirst et al., 2017; Vincent et al., 2023).

Despite significant genetic heterogeneity, ~67% of HSCR patients have mutations in genes of the *RET-EDNRB* gene regulatory network (GRN) (Tilghman et al., 2019). This GRN specifies bidirectional transcriptional feedback between *RET* and *EDNRB*, and the transcription factors *SOX10, GATA2, RARB,* and *NKX2-5,* as well as *GFRA1* and its ligand, *GDNF, EDN3*, the ligand for *EDNRB* and the ubiquitin ligase *CBL,* which degrades phosphorylated RET (Chatterjee and Chakravarti, 2019). To ascertain whether this feedback is associated with the iMN phenotype we observed, we quantified the expression of these genes and the changes arising from *Ret* deficiency. There is no expression of *Gdnf* and *Edn3* in iMN cells, as expected, since they are expressed and secreted from the surrounding mesenchyme (Baynash et al., 1994; Natarajan et al., 2002). *Ret* and its co-receptor *Gfra1* are downregulated 8-fold and 1.3-fold, respectively, while *Ednrb* is downregulated 6.2-fold (FDR<0.01 for all) in iMNs of +/Δmcs+9.7; +/CFP mice as compared to the wildtype (**Figure 4E**). Only *Ret* is significantly (FDR<0.01) downregulated in the Δmcs+9.7/Δmcs+9.7 gut by 1.28-fold leaving both *Gfra1* and *Ednrb* unaffected. Among the transcription factors controlling *Ret* and *Ednrb*, we did not observe expression of *Gata2* and *Nkx2-5* in iMN cells at E14.5 but *Sox10* is reduced by 12-fold and 6-fold (FDR<0.01 for both), respectively, in +/Δmcs+9.7; +/CFP and Δmcs+9.7/Δmcs+9.7 iMN cells, respectively. Thus even 5% and 58% loss of *Ret* expression has transcriptional changes affecting the core GRN disrupted in HSCR leading to observable cellular changes of the inhibitory motor neurons. In light of this observation, it is unsurprising that the

developmental trajectory leading to iMN formation is completely lost in *Ret* null embryos, as we have previously shown (Vincent et al., 2023).

Ret deficiency decreases proliferative capacity in iMNs

Reduction in proliferation capacity due to complete LoF of genes within the developing ENS, particularly those within the *Ret-Ednrb* GRN, are significant drivers of aganglionosis in the gut (Bergeron et al., 2016; Fujiwara et al., 2018; Vincent et al., 2023). Therefore, we asked whether similar but attenuated mechanisms operate to explain the iMN changes in Δmcs+9.7,+/ +,CFP embryos. Differential gene expression analysis at E14.5 with respect to both genotype and cell type identified 93 genes that are significantly altered in the iMNs of Δmcs+9.7,+/ +,CFP embryos, as compared to their wildtype littermates (**Supplementary table 5**). These include 10 genes involved in the cell cycle (*Cdkn1c, Ccnb2, Ccnb1, Ccna2, Cenpf, Cenpe, Cenpk, Ccnd1, Top2a, Cdk1*) which are >1.6-fold downregulated (FDR<0.01 for all) except for *Cdkn1c* and *Ccnd1*, which are 0.8- and 0.6-fold upregulated (FDR<0.01 for both), respectively (**Figure 4F**). Genes involved in DNA replication (*Gmnn, Mcm3, Mcm6, Mcm5, Mcm1*) and regulation of the cell cycle (*Rdcc, Mad2l1, Chek2, Rad51ap1*) were all downregulated between 1.4-fold and 2-fold (FDR<0.01 for all) (**Figure 4F and Supplementary table 6**). In the Δmcs+9.7/Δmcs+9.7 embryos all these 19 genes show a similar direction of change when compared to wildtype littermates but not all are statistically significant. Thus, both cell cycle occupancy and differentiation state, processes linked to proliferation, are disrupted in the double heterozygote as compared to wildtype embryos, specially affecting both a glial population with progenitor markers and iMNs. Our data demonstrate that collectively the observed gene expression changes and the subsequent cellular loss is restricted to the hindgut, as seen in our immunofluorescence data, in this model of *Ret* deficiency, modeling short segment HSCR (Alves et al., 2013; Tilghman et al., 2019).

Discussion

Numerous genomic studies of complex disorders have implicated both rare coding and common noncoding variants as causal genetic factors for their etiology (Chatterjee et al., 2016; Kapoor et al., 2014; Kelly et al., 2022). However, despite intensive research it

remains unclear how noncoding variants with small-to-modest genetic effects do affect the same *phenotype* as their cognate coding variants. Large effect coding variants or mutations can affect a rate-limiting gene's function critically and therefore lead to a phenotype directly. But how do noncoding variants affect the same phenotype when genomic evidence suggests that many such variants exert their effects only through cumulative action? We have previously hypothesized that this occurs only when the cumulative effect affects the same rate limiting step (a protein or a process modulated by several proteins) as the major coding mutations (Chakravarti and Turner, 2016). We now provide evidence that, at least for HSCR, quantitative changes in *Ret* gene expression and its protein affect the same gut developmental process in the same cells in the ENS at the same developmental time but do not affect all the target genes. The HSCR pathology (aganglionosis) results only when all target genes are affected as occurs through major qualitative changes in *Ret* gene expression and its protein.

The research described in this paper provides some clues as to why these two genetic architectures, coding and noncoding, have different quantitative properties: higher vs lower penetrance, and lower vs higher phenotypic variability, respectively. Despite affecting the same gut developmental program and the same GRN of genes, noncoding and coding *Ret* variants induce attenuated versus amplified responses of inhibitory motor neurons and a glial population with progenitor markers. Although such changes are now detectable at the single cell gene expression level, coding variants leads to phenotypic penetrance frequently while noncoding variants does so rarely. Why? A primary cause for this difference may be the stochastic nature of cell differentiation and proliferation, and *how many* cells are affected. Note that most but not all *RET* null heterozygotes have 100% penetrance (Emison et al., 2010). Thus, we believe that the number of cells which are affected, that is, have less than the optimum *Ret* gene expression of 50%, is larger in major coding mutations than in the common non-coding variants. Occasionally, the optimum is breached even with a non-coding variant but this occurs rarely (lower penetrance).

Our results also demonstrates that the 'aganglionosis' detected in human patients, and currently tested for in mouse models, from acetylcholinesterase staining, might arise from loss of *specific cell types* and is not a broad loss of all neuronal cells, as previously thought

(Furness, 2012). This increases the stochasticity of penetrance because smaller numbers of cells are at risk increasing the role of functional 'drift.' Thus, pathophysiological studies of HSCR might benefit from the use of additional histopathological markers to assess the phenotype in patients. This comment pertains to both the aganglionic, hypoganglionic and transition zone segments of the gut.

One of the yet unsolved observations in HSCR is the different lengths of the bowel (colon) affected by aganglionosis in different patients, with short segment disease being the most common (Badner et al., 1990). Although heritable, many families have mixed short and long segment disease: the genetic basis of this segment length variation remains unclear but at least in some families arises from the interaction between *Ret* coding and enhancer variants (Emison et al., 2010; Emison et al., 2005). Previously studied mouse models have either total intestinal aganglionosis from complete *Ret* deficiency (Uesaka et al., 2008), which is extremely rare in humans, or variable long segment disease from multigenic models which reflects the human condition only in some patients (Hirst et al., 2017; McCallion et al., 2003). Our double heterozygote mouse model with 42% *Ret* gene expression presents with aganglionosis only in the distal hindgut, thus most closely modeling short segment HSCR, the most common phenotype.

Finally, our data reaffirms previous observations that aganglionosis in HSCR animal models arises from proliferative defects in cells of the ENS. But why do all the cellular changes in these models affect only iMNs (Kuil et al., 2023; Spencer et al., 2021; Vincent et al., 2023)? One possible answer is that HSCR is basically a proliferative defect of iMNs and not a broad aganglionosis as previously assumed (Furness, 2012). But suspicion remains that the human cellular phenotype may be more complex than in the mouse, since recent studies of ENCDCs derived from HSCR patient-induced pluripotent stem cells demonstrates both gene expression and cell type composition that are different from mouse ENCDCs, with both committed glial progenitors (GP) and the neuronal progenitors (NP) absent in these patient-derived ENCDCs; this feature has not been recapitulated in mouse models (Li et al., 2023). Given the limited sample size and technical variations in deriving ENCDCs this observed differences needs to yet be conclusively proven. To investigate these

contrasting hypotheses directly, mouse models with human *RET* coding and noncoding normal and disease-associated haplotypes will prove to be instrumental.

Materials and Methods

Nomenclature of mutant mice

Our mouse models include disruptions in both the coding and enhancer regions of the same gene, an approach not commonly used in human genetic studies. To ensure clarity, as well as correspondence between the human and mouse orthologous elements, we provide the nomenclature table below, which we have consistently applied throughout the text and figures.

Ret coding genotype	*Ret* enhancer genotype	Genotype of mouse strain
+/+	+/+	wildtype or WT
+/+	+/deletion	+/+; +/Δmcs+9.7
+/+	deletion/deletion	+/+; Δmcs+9.7/Δmcs+9.7
+/deletion	+/deletion	+/CFP; +/Δmcs+9.7

Generation of Ret deficient mouse models

mcs+9.7 deletion mice: We used the following guide RNAs to delete the *RET* enhancer MCS+9.7 (chr10: 43,581,812–43,582,711; hg19) conserved in mice (mcs+9.7: 6:118,164,102-118,163,917; mmu39) with sequence identity 88%: Forward Guide: TCCTTCCGGCTTCTAGACAA (chr 6:118163913 – 118163932) and Reverse Guide: GCAGCAGCAACAGCTACTTG (chr 6:118164067 – 118164086). The guides were designed to delete a DNA fragment within the conserved sequence centered on the known Sox10 binding site. They were injected with Cas9 protein into one cell embryos by standard methods at the NYU transgenic core facility to delete the target DNA segment. We used the following primers to routinely genotype these mice: mcs+9.7 mKO-F: CACGTCCTGTCTCTTCCGTAG and mcs+9.7 mKO-R: AGCCTGTGAACGTGTTCTGC. Both the heterozygous and homozygous mcs+9.7 deletion (Δ) mice were born in the expected Mendelian proportions (**Supplementary Table 1-4**). These are referred to as Δmcs+9.7/+ and Δmcs+9.7/Δmcs+9.7, respectively.

Ret CFP knock-in mice (_Ret$^{CFP/+}$_; MGI:3777556): These mice were generated by crossing _Ret_fl/+ mice to β-actin-Cre mice to remove the RET9 cDNA: these mice were maintained on a C57BL/6 background and have been previously described in detail (Vincent et al., 2023). To generate double heterozygote mice deleted for both the _Ret_ enhancer and the _Ret_ coding sequence, mice Δmcs+9.7/Δmcs+9.7 mice were crossed to _CFP/+_ mice to produce Δmcs+9.7/Δmcs+9.7; +/+ and Δmcs+9.7/+; CFP/+ genotypes (the mutant sites are listed as mcs+9.7 and coding, respectively); all offspring were in expected Mendelian proportions (Supplementary Table 1). All mouse experiments were conducted in accordance with the NIH Guidance for the Care and Use of Laboratory Animals. All procedures were approved by the NYU School of Medicine Animal Care and Use Committee (Protocol number: s17-01779).

Dissection and dissociation of embryonic tissue
Foregut and hindgut tissue from Δmcs+9.7/Δmcs+9.7; +/+ and Δmcs+9.7/Δmcs+9.7; CFP/+ at E12.5 and E14.5 were dissociated into single-cell suspensions using Accumax (Sigma, USA). The cells were filtered serially through a 100 μm and 40 μm cell strainer, and centrifuged at 2,000 rpm for 5 m. The cell pellets were resuspended in 5% FBS, 4 mM EDTA in Leibovitz L-15 medium. This cell suspension was diluted to 20,000 cells and processed through the 10X Genomics GEM generator to create a standard 3' library as per the 10X Genomics standard protocol. These cells were sequenced at an average of $1 \times 10^5 \pm 10^4$ reads/cell.

Single cell gene expression (RNA-seq) analysis
Sequence files were processed through _CellRanger_ to generate the _barcodes, features_ and _matrix_ files. These files were processed through _Seurat_ (Stuart et al. 2019) to generate a matrix count file. Individual datasets for each genotype were then analyzed by normalizing and scaling the data followed by detecting high variable genes across cell types for downstream analysis using _sctransform_ in _Seurat_ (Hafemeister et al. 2019). Cells which met the following criteria were retained for further downstream analysis: (nUMI >= 500) & (nGene >= 250) & (log10GenesPerUMI > 0.80) and (mitoRatio < 0.20)). We only retained those genes which were detected in >10 cells. To eliminate technical differences between datasets and to perform comparative scRNA-seq analysis across experimental conditions

we utilized *Integration* analysis in *Seurat* which matched shared cell populations across datasets. These methods first identify cross-dataset pairs of cells that are in a matched biological state ('anchors'), before creating clusters of these cells to avoid bias. These are used as input to the uniform manifold approximation and projection (UMAP) dimensionality reduction tool to establish a biologically relevant two-dimensional embedding of the cells.

Single cell differential gene expression analysis

We used Seurat's *FindMarker* feature to perform differential expression by pseudo-bulking the samples either across genotypes or across cell clusters. We utilized "MAST": GLM-framework (Finak et al., 2015) that treats cellular detection rate as a covariate within *Seurat*.

Cell-type annotation

We annotated cell types by performing differential gene expression analysis by considering all markers with >1.5-fold change (FDR<0.05) in that cluster, as compared to all other clusters. These genes were analyzed for their GO terms using DAVID (Huang et al., 2007) and enriched GO terms (FDR <0.01 and containing >10 genes) were used to annotate the clusters. For ENS clusters, along with using unbiased cell type marker identification we also used previously identified markers for specific neuronal and glial cell types in the ENS (Elmentaite et al., 2021; Morarach et al., 2021; Vincent et al., 2023).

Immunofluorescence assays on whole mouse gut

Whole gut tissues, separated into stomach, foregut and hind gut, at E12.5 and E14.5 were dissected and washed in ice-cold PBS followed by fixation in 4% PFA at 4°C for 1 h. The fixed tissues were permeabilized and blocked in 5% normal donkey serum and 0.3% Triton-X for 1 h at room temperature (RT). The tissues were incubated with appropriate primary antibodies at 4°C overnight, washed with PBS, then incubated in appropriate secondary antibodies at 4°C overnight (see Dataset S12 for antibodies and dilutions). Tissues were washed in PBS and incubated with 0.2 µg/mL of DAPI (4′,6-diamidino-2-phenylindole) for 10 m at RT, followed by incubation for 20 m at RT with CUBIC-1 (16) diluted 1:10 with PBS. Samples were washed with PBS and mounted on Fisherbrand Superfrost Plus microscope slides with ProLong Gold Antifade mounting media and imaged using a Zeiss AxioVert Microscope.

Author Contributions

SC and AC conceived and designed the study. LEF and HRB created all mouse constructs. LEF and GG conducted single cell and immunofluorescence assays; SC and LEF analyzed the data. SC and AC wrote the manuscript. All authors approved the final version of the manuscript.

Declaration of Interests

The authors declare no conflicts of interest.

Acknowledgement
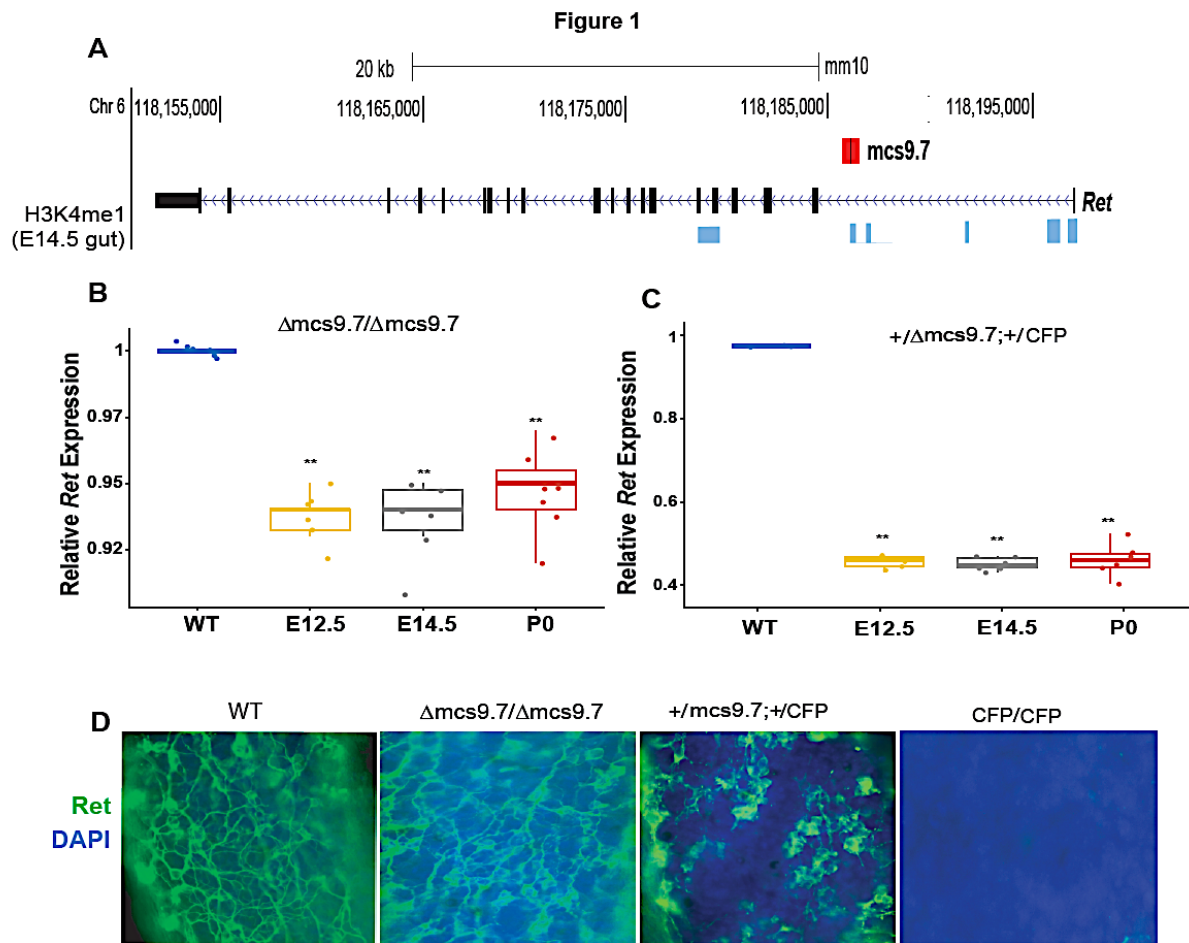
Figures

Figure 1: (A) 40kb mouse *Ret* locus (chr6:118,155,000-118,195,000; mm10) highlighting a 166bp deletion (Δmcs+9.7) of the conserved intronic *Ret* enhancer mcs+9.7. The chromatin around mcs+9.7 is both accessible and active as revealed by H3K27ac peaks in the E14.5 mouse GI tract (data from ENCODE). **(B)** Δmcs+9.7/+; Δmcs+9.7/+ homozygotes have a ~5% reduction in *Ret* gene expression in the mouse hindgut and foregut at E12.5 and E14.5. **(C)** Double heterozygote Δmcs+9.7/+; CFP/+ embryos have 45% *Ret* gene expression as compared to wildtype embryos at the same developmental times (** $p < 0.01$). **(D)** Immunofluorescence assays for Ret in +/+; +/+, Δmcs+9.7/+; Δmcs+9.7/+, and Δmcs+9.7/+; CFP/+ embryonic guts show reduction in *Ret* positive neurons in the hindgut of Δmcs+9.7/+; CFP/+ embryos at E14.5 followed by complete loss in +/+; CFP/CFP embryos.
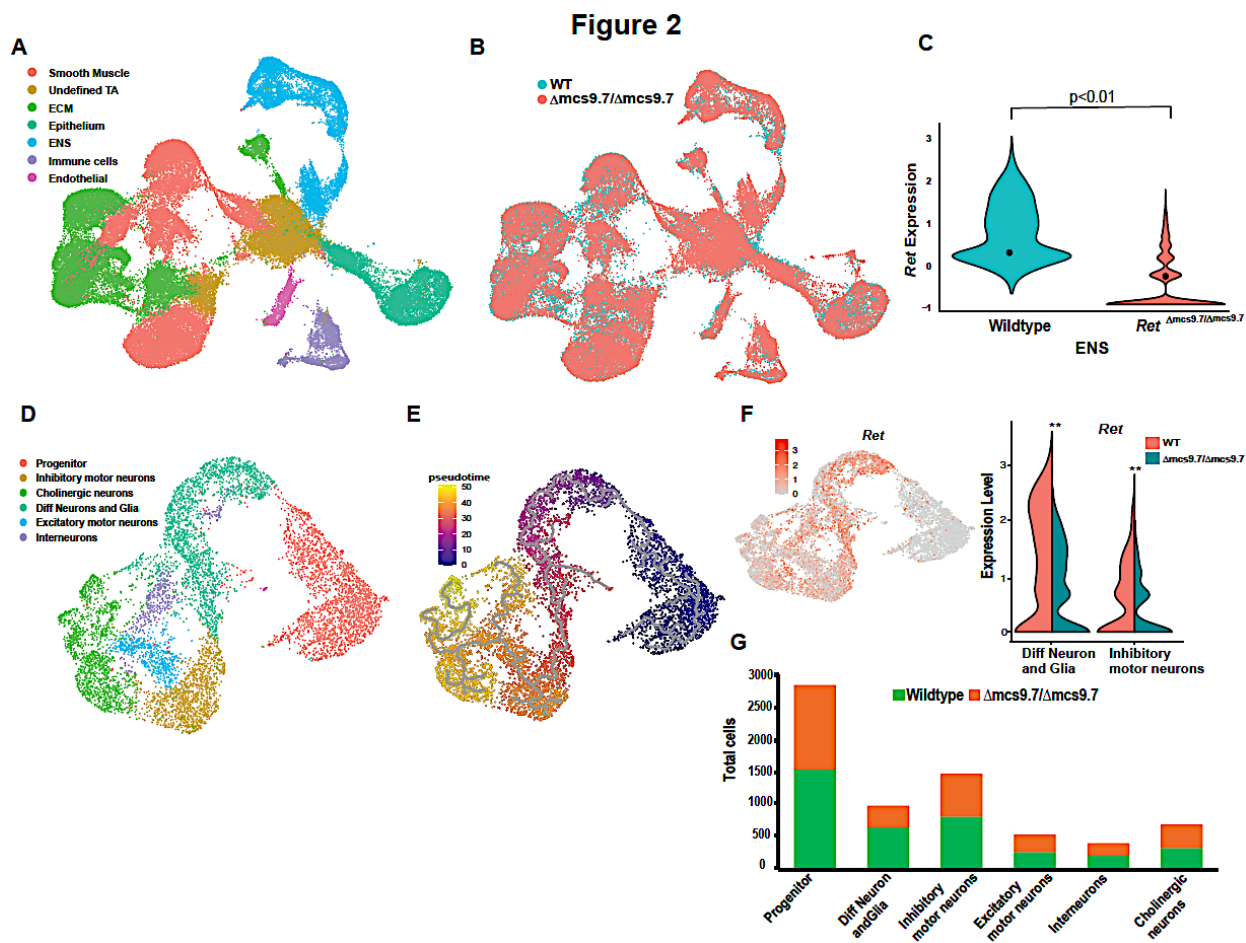
Figure 2: (A) UMAP embedding of the mouse GI tract at E14.5 colored by the 7 major cell types detected. **(B)** Homozygous loss of mcs+9.7 has no significant effect on any cell type at E14.5 (p=0.18; hypergeometric test), however **(C)** *Ret* gene expression is significantly diminished only in the ENS. **(D)** ENS cells cluster into 6 major cell types/states with **(E)** a clear differentiation pathway along a defined developmental trajectory (demonstrated using *Monocle*). **(F)** Loss of mcs9.7 activity significantly affects *Ret* gene expression in differentiating neurons, glia and inhibitory motor neurons (** p<0.01), however, **(G)** there are no losses in cell numbers in any ENS cell type/state in Δmcs+9.7/Δmcs+9.7 embryos, as compared to the wildtype.

Figure 3

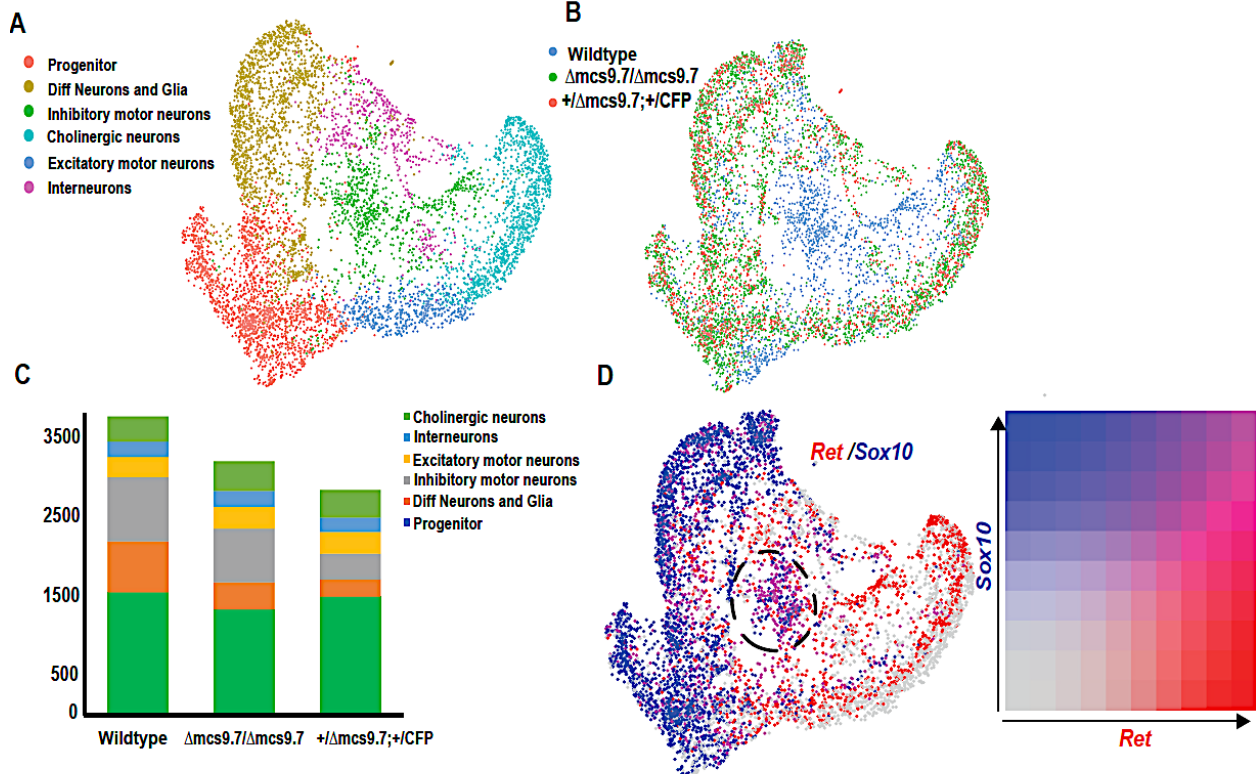**Figure 3: (A)** UMAP embedding of +/+; +/+, Δmcs+9.7/+; Δmcs+9.7/+, and Δmcs+9.7/+; CFP/+ ENS cells at E14.5 colored by the 6 major cell types detected. **(B)** Cluster 3 comprising inhibitory motor neurons has significantly fewer cells in both mutant genotypes from loss of *Ret* function in these cells. **(C)** There is significant cellular loss in both inhibitory motor neurons and differentiating neurons and glia in the Δmcs+9.7/+; CFP/+ GI tract as compared to the wildtype. **(D)** Among all ENS cells, inhibitory motor neurons, have the largest number (83%) of cells co-expressing *Ret* and *Sox10* (the transcription factor bound to mcs9.7) making it the primary site of action for the enhancer.
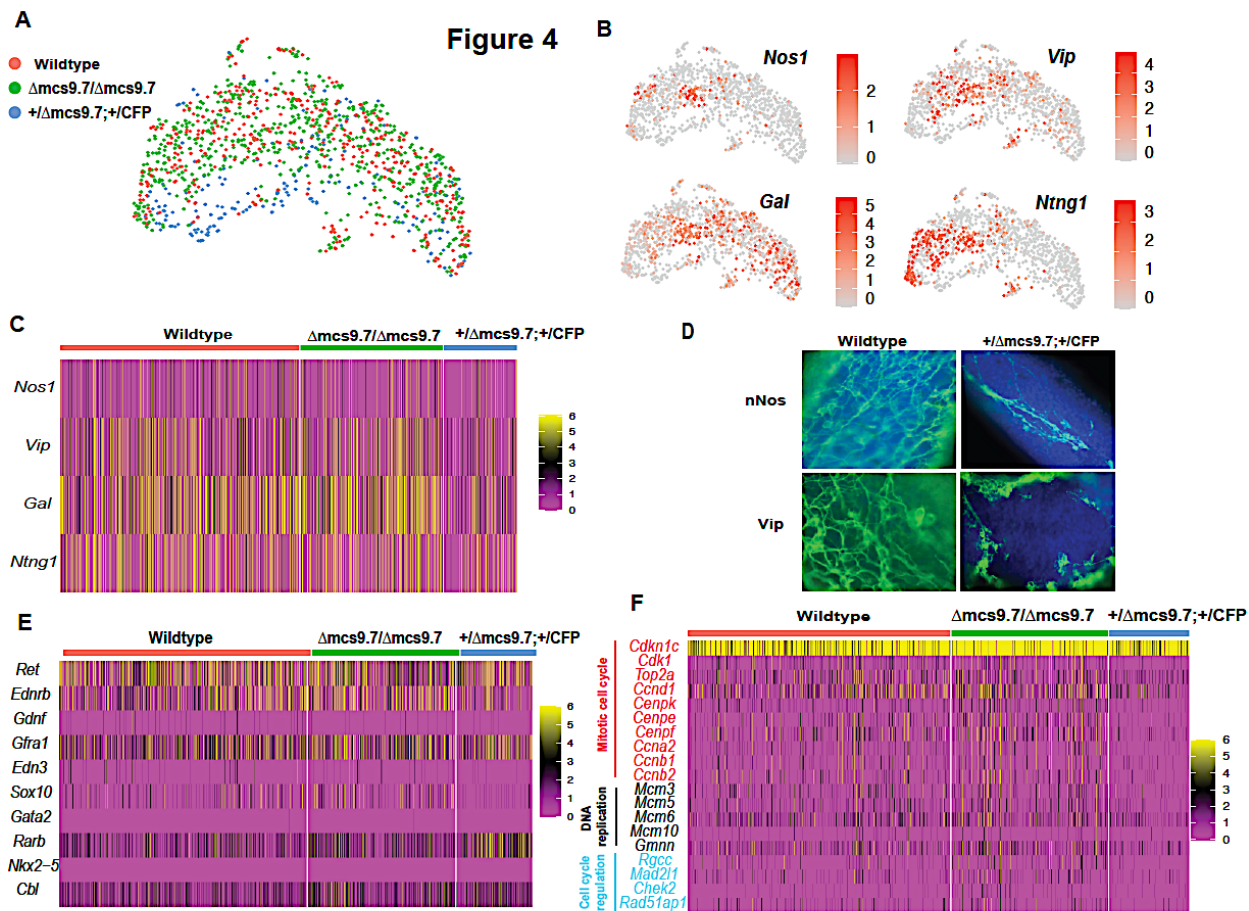
Figure 4: (A) UMAP embedding of +/+; +/+, Δmcs+9.7/+; Δmcs+9.7/+, and Δmcs+9.7/+; CFP/+ inhibitory motor neuron (iMNs) cells at E14.5 colored by genotype. **(B)** These cells have high expression of the classical iMN markers *Nos1, Vip, Gal* and *Ntng1* **(C)** which are significantly (FDR<0.01) downregulated in Δmcs+9.7/+; CFP/+ embryonic guts. **(D)** Immunofluorescence assays for nNOS and Vip in wildtype and Δmcs+9.7/+; CFP/+ embryos demonstrate severe reduction of these iMNs in the hindgut leading to cellular clumping of Vip positive neurons, a hallmark of proliferative and migratory defects. **(E)** Transcription of multiple genes of the *Ret-Ednrb* gene regulatory network is affected in both Δmcs+9.7/+; Δmcs+9.7/+, and Δmcs+9.7/+; CFP/+ embryonic guts. **(F)** 19 genes playing crucial roles in cell cycle regulation and DNA replication are differentially expressed in the Δmcs+9.7/+; CFP/+ embryonic gut, suggesting that the observed cellular loss is likely mediated by proliferative defects.

References

Alves, M.M., Sribudiani, Y., Brouwer, R.W., Amiel, J., Antinolo, G., Borrego, S., Ceccherini, I., Chakravarti, A., Fernandez, R.M., Garcia-Barcelo, M.M., Griseri, P., Lyonnet, S., Tam, P.K., van Ijcken, W.F., Eggen, B.J., te Meerman, G.J., Hofstra, R.M., 2013. Contribution of rare and common variants determine complex diseases-Hirschsprung disease as a model. Dev Biol 382, 320-329.

Badner, J.A., Sieber, W.K., Garver, K.L., Chakravarti, A., 1990. A genetic study of Hirschsprung disease. Am J Hum Genet 46, 568-580.

Baynash, A.G., Hosoda, K., Giaid, A., Richardson, J.A., Emoto, N., Hammer, R.E., Yanagisawa, M., 1994. Interaction of endothelin-3 with endothelin-B receptor is essential for development of epidermal melanocytes and enteric neurons. Cell 79, 1277-1285.

Bergeron, K.F., Nguyen, C.M., Cardinal, T., Charrier, B., Silversides, D.W., Pilon, N., 2016. Upregulation of the Nr2f1-A830082K12Rik gene pair in murine neural crest cells results in a complex phenotype reminiscent of Waardenburg syndrome type 4. Dis Model Mech 9, 1283-1293.

Bondurand, N., Sham, M.H., 2013. The role of SOX10 during enteric nervous system development. Dev Biol 382, 330-343.

Carrasquillo, M.M., McCallion, A.S., Puffenberger, E.G., Kashuk, C.S., Nouri, N., Chakravarti, A., 2002. Genome-wide association study and mouse model identify interaction between RET and EDNRB pathways in Hirschsprung disease. Nat Genet 32, 237-244.

Chakravarti, A., Turner, T.N., 2016. Revealing rate-limiting steps in complex disease biology: The crucial importance of studying rare, extreme-phenotype families. Bioessays 38, 578-586.

Chatterjee, S., Chakravarti, A., 2019. A gene regulatory network explains RET-EDNRB epistasis in Hirschsprung disease. Hum Mol Genet 28, 3137-3147.

Chatterjee, S., Fries, L.E., Yaacov, O., Hu, N., Berk-Rauch, H.E., Chakravarti, A., 2023. RET enhancer haplotype-dependent remodeling of the human fetal gut development program. PLoS Genet 19, e1011030.

Chatterjee, S., Kapoor, A., Akiyama, J.A., Auer, D.R., Lee, D., Gabriel, S., Berrios, C., Pennacchio, L.A., Chakravarti, A., 2016. Enhancer Variants Synergistically Drive Dysfunction of a Gene Regulatory Network In Hirschsprung Disease. Cell 167, 355-368 e310.

Chatterjee, S., Karasaki, K.M., Fries, L.E., Kapoor, A., Chakravarti, A., 2021. A multi-enhancer RET regulatory code is disrupted in Hirschsprung disease. Genome Res 31, 2199-2208.

Chatterjee, S., Nandakumar, P., Auer, D.R., Gabriel, S.B., Chakravarti, A., 2019. Gene- and tissue-level interactions in normal gastrointestinal development and Hirschsprung disease. Proc Natl Acad Sci U S A 116, 26697-26708.

Elmentaite, R., Kumasaka, N., Roberts, K., Fleming, A., Dann, E., King, H.W., Kleshchevnikov, V., Dabrowska, M., Pritchard, S., Bolt, L., Vieira, S.F., Mamanova, L., Huang, N., Perrone, F., Goh Kai'En, I., Lisgo, S.N., Katan, M., Leonard, S., Oliver, T.R.W., Hook, C.E., Nayak, K., Campos, L.S., Dominguez Conde, C., Stephenson, E., Engelbert, J., Botting, R.A., Polanski, K., van Dongen, S., Patel, M., Morgan, M.D., Marioni, J.C., Bayraktar, O.A., Meyer, K.B., He, X., Barker, R.A., Uhlig, H.H., Mahbubani, K.T., Saeb-Parsy, K., Zilbauer, M., Clatworthy, M.R., Haniffa, M., James, K.R., Teichmann, S.A., 2021. Cells of the human intestinal tract mapped across space and time. Nature 597, 250-255.

Emison, E.S., Garcia-Barcelo, M., Grice, E.A., Lantieri, F., Amiel, J., Burzynski, G., Fernandez, R.M., Hao, L., Kashuk, C., West, K., Miao, X., Tam, P.K., Griseri, P., Ceccherini, I., Pelet, A., Jannot, A.S., de Pontual, L., Henrion-Caude, A., Lyonnet, S., Verheij, J.B., Hofstra, R.M., Antinolo, G., Borrego, S., McCallion, A.S., Chakravarti, A., 2010. Differential contributions of rare and common, coding and noncoding Ret mutations to multifactorial Hirschsprung disease liability. Am J Hum Genet 87, 60-74.

Emison, E.S., McCallion, A.S., Kashuk, C.S., Bush, R.T., Grice, E., Lin, S., Portnoy, M.E., Cutler, D.J., Green, E.D., Chakravarti, A., 2005. A common sex-dependent mutation in a RET enhancer underlies Hirschsprung disease risk. Nature 434, 857-863.

Finak, G., McDavid, A., Yajima, M., Deng, J., Gersuk, V., Shalek, A.K., Slichter, C.K., Miller, H.W., McElrath, M.J., Prlic, M., Linsley, P.S., Gottardo, R., 2015. MAST: a flexible statistical framework for assessing transcriptional changes and characterizing heterogeneity in single-cell RNA sequencing data. Genome Biol 16, 278.

Fujiwara, N., Nakazawa-Tanaka, N., Miyahara, K., Arikawa-Hirasawa, E., Akazawa, C., Yamataka, A., 2018. Altered expression of laminin alpha1 in aganglionic colon of endothelin receptor-B null mouse model of Hirschsprung's disease. Pediatr Surg Int 34, 137-141.

Furness, J.B., 2012. The enteric nervous system and neurogastroenterology. Nat Rev Gastroenterol Hepatol 9, 286-294.

Grice, E.A., Rochelle, E.S., Green, E.D., Chakravarti, A., McCallion, A.S., 2005. Evaluation of the RET regulatory landscape reveals the biological relevance of a HSCR-implicated enhancer. Hum Mol Genet 14, 3837-3845.

Heanue, T.A., Pachnis, V., 2006. Expression profiling the developing mammalian enteric nervous system identifies marker and candidate Hirschsprung disease genes. Proc Natl Acad Sci U S A 103, 6919-6924.

Hirst, C.S., Stamp, L.A., Bergner, A.J., Hao, M.M., Tran, M.X., Morgan, J.M., Dutschmann, M., Allen, A.M., Paxinos, G., Furlong, T.M., McKeown, S.J., Young, H.M., 2017. Kif1bp loss in mice leads to defects in the peripheral and central nervous system and perinatal death. Sci Rep 7, 16676.

Huang, D.W., Sherman, B.T., Tan, Q., Collins, J.R., Alvord, W.G., Roayaei, J., Stephens, R., Baseler, M.W., Lane, H.C., Lempicki, R.A., 2007. The DAVID Gene Functional Classification Tool: a novel biological module-centric algorithm to functionally analyze large gene lists. Genome Biol 8, R183.

Jiang, Q., Arnold, S., Heanue, T., Kilambi, K.P., Doan, B., Kapoor, A., Ling, A.Y., Sosa, M.X., Guy, M., Jiang, Q., Burzynski, G., West, K., Bessling, S., Griseri, P., Amiel, J., Fernandez, R.M., Verheij, J.B., Hofstra, R.M., Borrego, S., Lyonnet, S., Ceccherini, I., Gray, J.J., Pachnis, V., McCallion, A.S., Chakravarti, A., 2015. Functional loss of semaphorin 3C and/or semaphorin 3D and their epistatic interaction with ret are critical to Hirschsprung disease liability. Am J Hum Genet 96, 581-596.

Kapoor, A., Auer, D.R., Lee, D., Chatterjee, S., Chakravarti, A., 2017. Testing the Ret and Sema3d genetic interaction in mouse enteric nervous system development. Hum Mol Genet 26, 1811-1820.

Kapoor, A., Sekar, R.B., Hansen, N.F., Fox-Talbot, K., Morley, M., Pihur, V., Chatterjee, S., Brandimarto, J., Moravec, C.S., Pulit, S.L., Consortium, Q.T.I.-I.G., Pfeufer, A., Mullikin, J., Ross, M., Green, E.D., Bentley, D., Newton-Cheh, C., Boerwinkle, E., Tomaselli, G.F., Cappola, T.P., Arking, D.E., Halushka, M.K., Chakravarti, A., 2014. An enhancer polymorphism at the cardiomyocyte intercalated disc protein NOS1AP locus is a major regulator of the QT interval. Am J Hum Genet 94, 854-869.

Kelly, T.N., Sun, X., He, K.Y., Brown, M.R., Taliun, S.A.G., Hellwege, J.N., Irvin, M.R., Mi, X., Brody, J.A., Franceschini, N., Guo, X., Hwang, S.J., de Vries, P.S., Gao, Y., Moscati, A., Nadkarni, G.N., Yanek, L.R., Elfassy, T., Smith, J.A., Chung, R.H., Beitelshees, A.L., Patki, A., Aslibekyan, S., Blobner, B.M., Peralta, J.M., Assimes, T.L., Palmas, W.R., Liu, C., Bress, A.P., Huang, Z., Becker, L.C., Hwa, C.M., O'Connell, J.R., Carlson, J.C., Warren, H.R., Das, S., Giri, A., Martin, L.W., Craig Johnson, W., Fox, E.R., Bottinger, E.P., Razavi, A.C., Vaidya, D., Chuang, L.M., Chang, Y.C., Naseri, T., Jain, D., Kang, H.M., Hung, A.M., Srinivasasainagendra, V., Snively, B.M., Gu, D., Montasser, M.E., Reupena, M.S., Heavner, B.D., LeFaive, J., Hixson, J.E., Rice, K.M., Wang, F.F., Nielsen, J.B., Huang, J., Khan, A.T., Zhou, W., Nierenberg, J.L., Laurie, C.C., Armstrong, N.D., Shi, M., Pan, Y., Stilp, A.M., Emery, L., Wong, Q., Hawley, N.L., Minster, R.L., Curran, J.E., Munroe, P.B., Weeks, D.E., North, K.E., Tracy, R.P., Kenny, E.E., Shimbo, D., Chakravarti, A., Rich, S.S., Reiner, A.P., Blangero, J., Redline, S., Mitchell, B.D., Rao, D.C., Ida Chen, Y.D., Kardia, S.L.R., Kaplan, R.C., Mathias, R.A., He, J., Psaty, B.M., Fornage, M., Loos, R.J.F., Correa, A., Boerwinkle, E., Rotter, J.I., Kooperberg, C., Edwards, T.L., Abecasis, G.R., Zhu, X., Levy, D., Arnett, D.K., Morrison,

A.C., Samoan Obesity, L., Genetic Adaptations Study Group, d.d.N.T.-O.f.P.M.T.C., 2022. Insights From a Large-Scale Whole-Genome Sequencing Study of Systolic Blood Pressure, Diastolic Blood Pressure, and Hypertension. Hypertension 79, 1656-1667.

Kuil, L.E., Kakiailatu, N.J.M., Windster, J.D., Bindels, E., Zink, J.T.M., van der Zee, G., Hofstra, R.M.W., Shepherd, I.T., Melotte, V., Alves, M.M., 2023. Unbiased characterization of the larval zebrafish enteric nervous system at a single cell transcriptomic level. iScience 26, 107070.

Lasrado, R., Boesmans, W., Kleinjung, J., Pin, C., Bell, D., Bhaw, L., McCallum, S., Zong, H., Luo, L., Clevers, H., Vanden Berghe, P., Pachnis, V., 2017. Lineage-dependent spatial and functional organization of the mammalian enteric nervous system. Science 356, 722-726.

Li, Z., Lui, K.N., Lau, S.T., Lai, F.P., Li, P., Chung, P.H., Wong, K.K., Tam, P.K., Garica-Barcelo, M.M., Hui, C.C., Sham, P.C., Ngan, E.S., 2023. Transcriptomics of Hirschsprung disease patient-derived enteric neural crest cells reveals a role for oxidative phosphorylation. Nat Commun 14, 2157.

McCallion, A.S., Stames, E., Conlon, R.A., Chakravarti, A., 2003. Phenotype variation in two-locus mouse models of Hirschsprung disease: tissue-specific interaction between Ret and Ednrb. Proc Natl Acad Sci U S A 100, 1826-1831.

Morarach, K., Mikhailova, A., Knoflach, V., Memic, F., Kumar, R., Li, W., Ernfors, P., Marklund, U., 2021. Diversification of molecularly defined myenteric neuron classes revealed by single-cell RNA sequencing. Nat Neurosci 24, 34-46.

Natarajan, D., Marcos-Gutierrez, C., Pachnis, V., de Graaff, E., 2002. Requirement of signalling by receptor tyrosine kinase RET for the directed migration of enteric nervous system progenitor cells during mammalian embryogenesis. Development 129, 5151-5160.

Paratore, C., Eichenberger, C., Suter, U., Sommer, L., 2002. Sox10 haploinsufficiency affects maintenance of progenitor cells in a mouse model of Hirschsprung disease. Hum Mol Genet 11, 3075-3085.

Schuchardt, A., D'Agati, V., Larsson-Blomberg, L., Costantini, F., Pachnis, V., 1994. Defects in the kidney and enteric nervous system of mice lacking the tyrosine kinase receptor Ret. Nature 367, 380-383.

Spencer, N.J., Travis, L., Wiklendt, L., Costa, M., Hibberd, T.J., Brookes, S.J., Dinning, P., Hu, H., Wattchow, D.A., Sorensen, J., 2021. Long range synchronization within the enteric nervous system underlies propulsion along the large intestine in mice. Commun Biol 4, 955.

Tilghman, J.M., Ling, A.Y., Turner, T.N., Sosa, M.X., Krumm, N., Chatterjee, S., Kapoor, A., Coe, B.P., Nguyen, K.H., Gupta, N., Gabriel, S., Eichler, E.E., Berrios, C., Chakravarti,

A., 2019. Molecular Genetic Anatomy and Risk Profile of Hirschsprung's Disease. N Engl J Med 380, 1421-1432.

Trapnell, C., Cacchiarelli, D., Grimsby, J., Pokharel, P., Li, S., Morse, M., Lennon, N.J., Livak, K.J., Mikkelsen, T.S., Rinn, J.L., 2014. The dynamics and regulators of cell fate decisions are revealed by pseudotemporal ordering of single cells. Nat Biotechnol 32, 381-386.

Uesaka, T., Nagashimada, M., Yonemura, S., Enomoto, H., 2008. Diminished Ret expression compromises neuronal survival in the colon and causes intestinal aganglionosis in mice. J Clin Invest 118, 1890-1898.

Vincent, E., Chatterjee, S., Cannon, G.H., Auer, D., Ross, H., Chakravarti, A., Goff, L.A., 2023. Ret deficiency decreases neural crest progenitor proliferation and restricts fate potential during enteric nervous system development. Proc Natl Acad Sci U S A 120, e2211986120.

Yoshimaru, K., Matsuura, T., Yanagi, Y., Obata, S., Takahashi, Y., Kajihara, K., Ohmori, A., Irie, K., Hino, Y., Shibui, Y., Tamaki, A., Kohashi, K., Oda, Y., Taguchi, T., 2021. Reevaluation of concurrent acetylcholinesterase and hematoxylin and eosin staining for Hirschsprung's disease. Pediatr Int 63, 1095-1102.